Received: 14 July 2020 | Revised: 2 September 2020 | Accepted: 2 September 2020

DOI: 10.1111/tbed.13823

ORIGINAL ARTICLE

Transboundary and Emerging Diseases WILEY

Shuni virus-induced meningoencephalitis after experimental infection of cattle

Franziska Sick[1] | Angele Breithaupt[2] | Natalia Golender[3] | Velizar Bumbarov[3] | Martin Beer[1] | Kerstin Wernike[1]

[1]Institute of Diagnostic Virology, Friedrich-Loeffler-Institut, Greifswald-Insel Riems, Germany

[2]Department of Experimental Animal Facilities and Biorisk Management, Friedrich-Loeffler-Institut, Greifswald-Insel Riems, Germany

[3]Department of Virology, Kimron Veterinary Institute, Bet Dagan, Israel

Correspondence
Kerstin Wernike, Institute of Diagnostic Virology, Friedrich-Loeffler-Institut, 17493 Greifswald - Insel Riems, Germany.
Email: kerstin.wernike@fli.de

Funding information
German Federal Ministry of Food and Agriculture (BMEL) through the Federal Office for Agriculture and Food, Grant/Award Number: 281B101816; Marie Skłodowska-Curie Actions (MSCA) Innovative Training Networks (ITN) H2020-MSCA-ITN-2016, Grant/Award Number: 721367

Abstract

Shuni virus (SHUV), an insect-transmitted orthobunyavirus of the Simbu serogroup within the family *Peribunyaviridae*, may induce severe congenital malformations when naïve ruminants are infected during gestation. Only recently, another clinical presentation in cattle, namely neurological disease after postnatal infection, was reported. To characterize the course of the disease under experimental conditions and to confirm a causal relationship between the virus and the neurological disorders observed in the field, six calves each were experimentally inoculated (subcutaneously) with two different SHUV strains from both clinical presentations, that is encephalitis and congenital malformation, respectively. Subsequently, the animals were monitored clinically, virologically and serologically for three weeks. All animals inoculated with the 'encephalitis strain' SHUV 2162/16 developed viremia for three to four consecutive days, seroconverted, and five out of six animals showed elevated body temperature for up to three days. No further clinical signs such as neurological symptoms were observed in any of these animals. However, four out of six animals developed a non-suppurative meningoencephalitis, characterized by perivascular cuffing and glial nodule formation. Moreover, SHUV genome could be visualized in brain tissues of the infected animals by in situ hybridization. In contrast to the 'encephalitis SHUV strain', in animals subcutaneously inoculated with the strain isolated from a malformed newborn (SHUV 2504/3/14), which expressed a truncated non-structural protein NSs, a major virulence factor, no viremia or seroconversion, was observed, demonstrating an expected severe replication defect of this strain in vivo. The lack of viremia further indicates that virus variants evolving in malformed foetuses may represent attenuated artefacts as has been described for closely related viruses. As the neuropathogenicity of SHUV could be demonstrated under experimental conditions, this virus should be included in differential diagnosis for encephalitis in ruminants, and cattle represent a suitable animal model to study the pathogenesis of SHUV.

KEYWORDS

cattle, encephalitis, pathogenesis, Peribunyaviridae, Shuni virus, Simbu serogroup

1 | INTRODUCTION

The insect-transmitted Shuni virus (SHUV) is a member of the Simbu serogroup within the family *Peribunyaviridae*, genus *Orthobunyavirus* (Plyusnin & Elliott, 2011). Besides SHUV, several viruses of veterinary importance such as Akabane virus (AKAV) or Schmallenberg virus (SBV) are assigned to the Simbu serogroup. SHUV was firstly isolated in Nigeria in 1960 from apparently healthy cattle (Causey et al., 1972), and, thereafter, it was also detected in further African countries. In 2014, the virus was reported for the first time outside of the African continent, namely in the Middle East, where it was isolated from malformed lambs in Israel (Golender et al., 2015). In the following years, SHUV was repeatedly detected in aborted and/or malformed calves or lambs in this country (Golender et al., 2018); hence, the virus established an endemic status in Israel. As SHUV is transmitted by biting midges (genus *Culicoides*) (Möhlmann et al., 2018), which occur worldwide, a further spread of the virus into hitherto unaffected regions seems very likely.

In general, Simbu serogroup virus infections can cause two different types of clinical manifestation in ruminants. Acute infections of animals of all age groups are either asymptomatic or mild, associated with unspecific signs like fever, diarrhoea or loss in milk yield for a few days (Kirkland, 2015; Wernike et al., 2015). However, when naïve dams are infected during a critical phase of gestation, severe congenital defects referred to as arthrogryposis-hydranencephaly syndrome (AHS), abortion, premature birth, mummification or stillbirth can occur (Beer & Wernike, 2019; Kirkland, 2015; Wernike et al., 2015).

For SHUV and AKAV, another clinical presentation is described after natural infection. In rare cases, some strains of AKAV may induce encephalitis in newborn calves and the Iriki strain has been occasionally associated with encephalitis in young and adult cattle (Miyazato et al., 1989). Only recently, severe neurological signs have been described in young cattle naturally infected with SHUV (Golender et al., 2019). However, for SHUV the pathogenesis of this clinical presentation is largely unknown. In addition to the disease induced in ruminants, SHUV has also been associated with neurological diseases in horses in South Africa (van Eeden et al., 2012). Apart from animals, SHUV was isolated from a febrile child in Nigeria (Moore et al., 1975) and specific antibodies were found in veterinarians in South Africa. Hence, a zoonotic potential cannot be excluded; however, no clear histories of disease compatible with SHUV infections could be determined from antibody-positive veterinarians (van Eeden et al., 2014).

Similar to other orthobunyaviruses, SHUV is spherical, about 100 nm in diameter and comprises a tri-partite single-stranded negative-sense RNA genome that encodes for four structural and two non-structural proteins (Walter & Barr, 2011). The small (S) genomic segment encodes for the nucleocapsid protein N and in an overlapping reading frame for the non-structural protein NSs. The medium (M) segment encodes for the glycoproteins Gn and Gc, and the non-structural protein NSm, and the large (L) segment encodes for the RNA dependent RNA polymerase (Walter & Barr, 2011). The NSs protein acts as an interferon antagonist and induces a shut-off of protein synthesis in mammalian cells; hence, it represents a major virulence factor in vertebrate hosts (Elliott & Blakqori, 2011). For the insect vector, the function of both non-structural proteins remains largely unknown.

From ovine and bovine samples collected during the recent SHUV outbreak in Israel, infectious viruses could be successfully isolated (Golender et al., 2015, 2019). Sequence analysis revealed that the amino acid (aa) sequences of the viral N protein are highly conserved. Israeli SHUVs show an overall identity of 99.3 to 100%, however, when compared to the more ancient African sequences, aa identity decreases to about 90.5% (Golender et al., 2016). Nevertheless, single point mutations in the nucleotide sequences found in Israeli isolates from foetal brains led to changes in aa sequence or resulted in stop codons. A SHUV isolate with mutations leading to a truncated NSs protein showed a loss of function of the NSs protein in vitro (Golender et al., 2016). Whether this mutation also effects the function in vivo remains unknown.

In the present study, cattle were experimentally inoculated with two recent Israeli SHUV isolates and clinically, virologically, serologically and pathologically investigated to characterize the course of the disease. The first isolate represented the virus displaying a truncated, non-functional NSs protein, and the second isolate was obtained from acutely infected cattle showing neurological symptoms including compulsive circling, ataxia, swallowing difficulties and dysstasia.

2 | MATERIALS AND METHODS

2.1 | Viruses

Viruses from both previously described clinical pictures, namely encephalitis and congenital malformation, were selected. The first virus strain 'SHUV 2162/16' was isolated on Vero cells from the brain homogenate of a heifer showing neurological symptoms such as compulsive circling, ataxia, swallowing difficulties and later on dysstasia and recumbency (Golender et al., 2019). The second virus strain 'SHUV 2504/3/14' was obtained from the brain of a malformed, aborted sheep foetus using suckling mice and Vero cells (Golender et al., 2015). The latter isolate expresses a truncated NSs protein due to a stop codon in the NSs open reading frame (Golender et al., 2016). Both isolates were passaged once each on *Culicoides sonorensis* cells (KC, L1062, collection of cell lines in veterinary medicine (CCLV), Friedrich-Loeffler-Institut, Greifswald-Insel Riems, Germany) and baby hamster kidney cells (BHK 21, L0164 CCLV).

2.2 | Animals and experimental design

Fourteen cattle between 7 and 11 months of age (13 females, one castrated male) were obtained from a commercial supplier and rehoused to an insect-proof high containment stable. The animals

were kept in two infection groups of six cattle each, and the two remaining negative-control animals were kept separately. Before the experimental inoculation, sera of all animals were tested by a commercially available SBV antibody ELISA (ID Screen Schmallenberg virus competition multispecies; IDvet, Grabels, France) that also detects antibodies against several other Simbu serogroup viruses (Oluwayelu et al., 2018; Wernike et al., 2017) and by a microneutralization test against SHUV isolate 2162/16. All sera tested negative.

Six animals each were subcutaneously injected with 1 ml containing 10^6 $TCID_{50}$/mL of SHUV strain 2162/16 (cattle numbers C1 to C6) or strain 2504/3/14 (cattle C7 to C12), respectively. The two control animals (C13 and C14) were subcutaneously injected with 1 ml of phosphate-buffered saline (PBS). Throughout the study, the animals were monitored daily by veterinarians using a clinical scoring system (depending on the severity of clinical signs, up to 3 points were awarded for changes in activity, posture, gait and feeding behaviour). Rectal body temperatures were measured daily.

Whole blood and serum samples were collected daily for 10 days, on day 14 and on day 21. After three weeks, all animals were killed and tissue samples were collected (duodenum, jejunum, ileum (including Peyer's patches), caecum, rectum, spleen, tonsil, mesenteric, tracheobronchial, mandibular and retropharyngeal lymph nodes, spinal cord, cerebrum and cerebellum, liver, kidney, heart, ovary, muscle).

The experimental protocol was evaluated by a state ethics commission and approved by the competent authority (permission number LALLF M-VTSD/7221.3–2-010/18).

2.3 | RNA extraction and real-time RT-PCR

Tissue samples were homogenized in 1 ml of Modified Eagle Medium (MEM) using a TissueLyzer (Qiagen, Hilden, Germany). Total RNA from the tissue homogenates, serum and whole blood samples was extracted using the King Fisher 96 Flex purification system (Thermo Scientific, Braunschweig, Germany) in combination with the NucleoMag Vet kit (Macherey-Nagel, Düren, Germany) according to the manufacturers' instructions. The extracts were subsequently tested for SHUV genome using an S-segment-based generic Simbu serogroup real-time RT-PCR (Golender et al., 2018). To control for efficient RNA extraction and amplification, thereby avoiding false-negative results, an internal control based on the beta-actin gene was additionally tested (Toussaint et al., 2007).

2.4 | Serology

The sera collected at weekly intervals were heat inactivated at 56°C for 30 min and analysed by a standard microneutralization test against the virus isolate used for inoculation, sera obtained from the control animals were tested against both isolates. Each serum was tested in quadruplicate. The serum samples were first diluted in MEM in a 1/5 ratio and titrated in two-fold dilutions. Subsequently, 50 µl of the diluted sera were incubated with 50 µl of MEM containing approximately 100 $TCID_{50}$ of SHUV, which was confirmed by performing back-titrations, in microtiter plates for 2 hr at 37°C. Thereafter, 100µl of a BHK21 cell suspension was added to the virus-serum mixture and incubated at 37°C for 3 to 4 days. Evaluation was done by assessing the cytopathic effect. The antibody titres were calculated as ND_{50} (neutralization dose 50%) according to Behrens and Kaerber (Behrens & Kärber, 1934).

In addition, the sera were tested in an indirect immunofluorescence assay against the virus isolate used for inoculation. Sera of the control animals were tested against both SHUV strains. As antigen matrix, Vero cells (VERO 76, L0228 CCLV) were cultivated in 96-well microtiter plates. Odd-numbered columns were either infected with SHUV strain 2162/16 or 2504/3/14, while even numbered columns were left uninfected to control for unspecific reactions of the sera. After a 24-hr incubation period at 37°C, cells were heat-fixed at 80°C for 2 hr.

The cells were incubated with the sera pre-diluted in PBS (serial dilution of 1/50 to 1/400 in steps of 50). Binding of serum antibodies to the SHUV-infected and uninfected cells was visualized by adding a fluorescein-labelled secondary anti-bovine antibody (Anti-Bovine IgG (whole molecule)-FITC produced in rabbit, Sigma life sciences, St. Louis, USA). The assay was evaluated using a fluorescence microscope (Eclipse Ti-U, Nikon, Melville, USA). A comparison of infected and uninfected cells facilitated to exclude unspecific reactions.

Moreover, the sera were tested by a commercially available SBV antibody ELISA (ID Screen Schmallenberg virus competition multispecies; IDvet, Grabels, France) that also detects antibodies against several other Simbu serogroup viruses (Oluwayelu et al., 2018; Wernike et al., 2017).

2.5 | Autopsy, histopathology and in situ hybridization

Full autopsies were performed on all animals according to a standard protocol. The brain and cervical spinal cord were collected and fixed in 10% neutral-buffered formalin. Coronal sections of the following brain regions were processed: cortex (frontal and parietal lobe), the periventricular area of the lateral ventricle (region of caudate nucleus), hippocampus region, cerebral aqueduct with periaqueductal grey and white matter, cerebellum and cervical spinal cord. Tissues were embedded in paraffin, cut at three µm and stained with haematoxylin and eosin for light microscopic analyses. Meningeal infiltrates and perivascular immune cell cuffing in the grey and white matter were evaluated using a semi-quantitative scoring system, considering the most severely affected area: no lesion; up to three cell layers = mild; 4–9 cell layers = moderate; ≥10 layers = severe. The presence of glial nodules was recorded for the grey and white matter: no nodules, few (one focus per 20× field), multiple (two to three foci), abundant (≥ four foci).

Consecutive slides of areas with the most abundant inflammation were processed for immunohistochemistry. T-cell, B-cell and microglia/macrophage markers were applied, apoptosis was detected

by active-caspase-3 labelling and potential astrogliosis was tested by using glial fibrillary acidic protein (GFAP) immunohistochemistry, according to standardized procedures (see Table 1). Non-specific antibody binding was blocked with undiluted goat normal serum for 30 min at room temperature. Immunolabeling was visualized by 3-amino-9-ethylcarbazole substrate (AEC, Dako, Agilent, Santa Clara, CA, USA) producing a red-brown signal, and sections were counter-stained with Mayer's haematoxylin.

On additional consecutive sections, conventional staining protocols were applied, including Luxol Fast Blue Cresyl Violet for detection of myelin sheaths and Nissl substance, von Kossa stain to show mineralization and Prussian blue reaction for demonstration of ferric iron, indicating hemosiderin.

RNA in situ hybridization for the detection of SHUV RNA in brain tissue sections was performed with the RNAScope® 2–5 HD Reagent Kit-Red (ACD, Advanced Cell Diagnostics, Newark, CA) according to the manufacturer's instructions. For hybridization, RNAScope® probes were custom-designed for the nucleocapsid protein. The specificity of the probes was verified using a positive control probe peptidylprolyl isomerase B (cyclophilin B, ppib) and a negative control probe dihydrodipicolinate reductase (DapB). Histopathology and RNAScope® interpretation were performed by a board-certified pathologist (DiplECVP).

3 | RESULTS

3.1 | Clinical manifestation

After inoculation, all animals were monitored daily for clinical signs. All cattle inoculated with SHUV strain 2162/16 except for C3 showed elevated rectal body temperatures (>39.5°C), reaching values as high as 40.4°C (C1), for one to three days starting at the earliest at day four post-infection (dpi). The course of fever varied markedly between the individual animals of this group (Figure 1). In contrast, the body temperature of the animals inoculated with SHUV strain 2504/3/14 and of the uninfected control cattle remained in a normal temperature range (<39.5°C) throughout the study (Figure 1). Further clinical signs such as neurological changes were never observed in any animal.

3.2 | Detection of viral genome

Viral genome was detected by real-time RT-PCR in the blood of all animals inoculated with SHUV strain 2162/16 for three to four consecutive days starting two or three days after infection (Figure 2). No remarkable differences between whole blood and serum samples were observed. The whole blood and serum samples of animals inoculated with strain 2504/3/14 and of the control animals tested negative for all animals at all time points.

From the diverse panel of tissue samples collected during autopsy, only lymphatic and nervous tissue samples of the animals inoculated with strain 2162/16 tested positive by real-time RT-PCR. In samples collected from cattle C1, SHUV RNA was found in the spleen (quantification cycle (Cq) value: 38.7), the spinal cord (Cq 35.7) and in the cerebellum (Cq 34.8). In animal C2, SHUV RNA was detected only in the cerebrum (Cq 39.4), while in C3 viral RNA could be detected only in the spleen (Cq 33.5). In cattle C4, viral RNA was found in the spinal cord (Cq 35.1), cerebellum (Cq 32.8) and cerebrum (Cq 33.8). In cattle C6, viral RNA was found in spleen (Cq 35.5), spinal cord (Cq 38.5) and cerebellum (Cq 34.3). No viral genome could be detected in any other tissue sample of the aforementioned cattle. Animal C5, as well as all cattle inoculated with SHUV strain 2504/3/14 and the uninfected control animals tested negative by real-time RT-PCR in every tissue sample.

3.3 | Antibody detection

On the day of inoculation, the sera of all animals reacted negative in the neutralization test. All animals inoculated with SHUV strain

TABLE 1 Immunohistochemical markers and applications. HIER: heat-induced epitope retrieval, RT: room temperature

Marker	Antibody	Pre-treatment	Secondary reagents
CD79a	Mouse anti-CD79A (LifeSpan BioSciences, Seattle, WA, #LS-B8330), 1/50, overnight	HIER, 10mM Tris/ 1mM EDTA buffer pH 9.0, 20 min	Dako EnVision+ System- HRP Labelled Polymer Anti-mouse, 30 min (Dako, Agilent, Santa Clara, CA, USA)
CD3	Rabbit anti-CD3 polyclonal (Dako, #A045229–2), 1/100, overnight	HIER, 10mM Tris/ 1mM EDTA buffer pH 9.0, 20 min	Dako EnVision+ System- HRP Labelled Polymer Anti-rabbit, 30 min
Iba–1	Rabbit anti Iba1 (FUJIFILM Wako Pure Chemical Corporation, Osaka, Japan, # 019–19741), 1/800, overnight	HIER, Citrate buffer pH 6.0, for 20 min	Dako EnVision+ System- HRP Labelled Polymer Anti-rabbit, 30 min
GFAP	Rabbit anti GFAP (abcam, Cambridge, UK, #ab16997), 1/200, overnight	HIER, Citrate buffer pH 6.0, for 20 min	Dako EnVision+ System- HRP Labelled Polymer Anti-rabbit, 30 min
active caspase 3	Rabbit anti-active caspase 3 (Promega, Madison, WI, USA, #G7481), 1/200, overnight	No pre-treatment	Anti-Rabbit IgG Biotinylated, 1/200, 30 min. RT; and ABC Kit Vectastain Elite PK 6100, 30 min (Vector Laboratories, Burlingame, CA, USA)

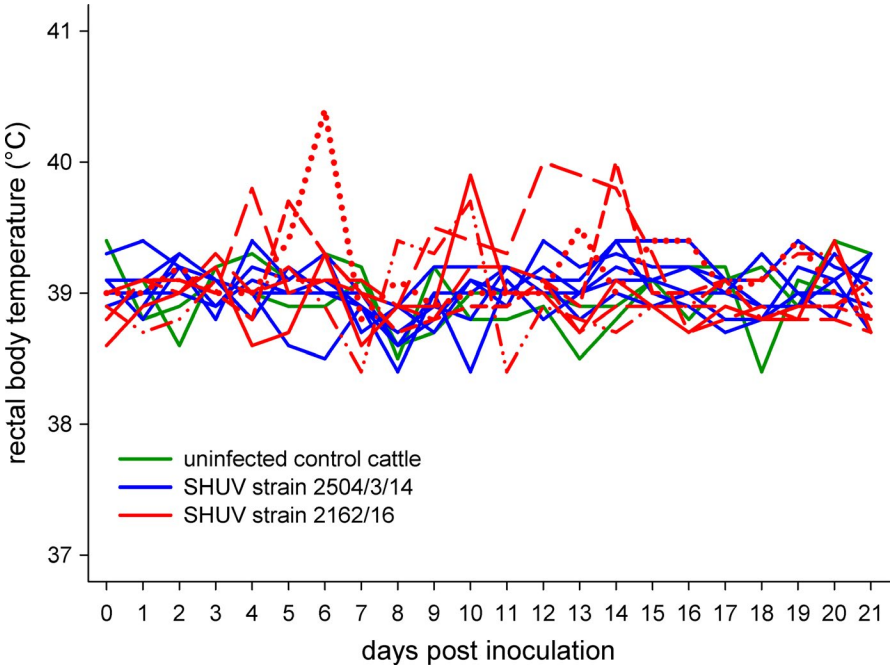

FIGURE 1 Rectal body temperature of cattle inoculated with either Shuni virus strain 2162/16 (red) or 2504/3/14 (blue). Uninfected control animals are shown in green [Colour figure can be viewed at wileyonlinelibrary.com]

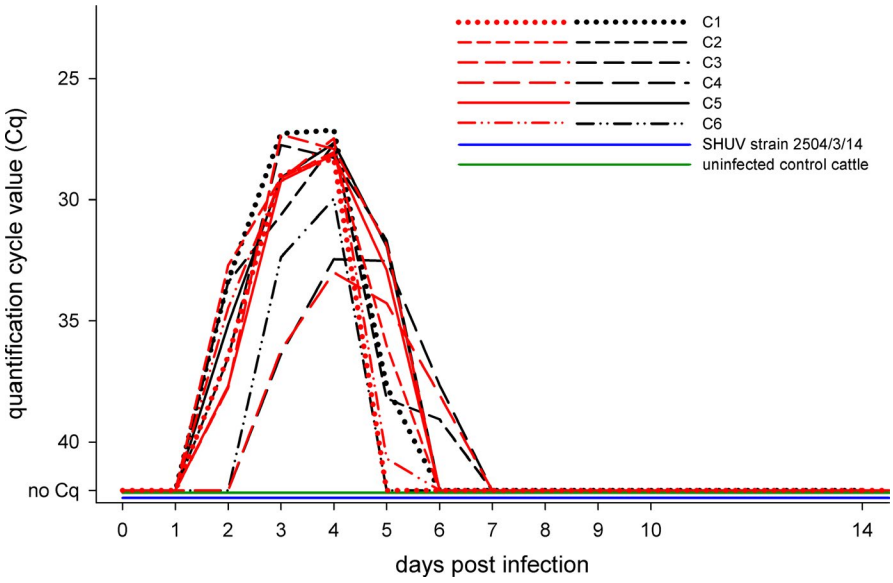

FIGURE 2 Real-time RT-PCR results for whole blood (shown in black) and serum samples (shown in red). Samples taken from the same animal are depicted by the identical line type. No Shuni virus RNA was detected in C7 - C12, which were inoculated with strain 2504/3/14, or in the uninfected control animals at any time [Colour figure can be viewed at wileyonlinelibrary.com]

2162/16 seroconverted; neutralizing antibodies could be detected from day seven onwards, reaching titres as high as 1/320 at 14 or 21 dpi (Table 2). In the group that was inoculated with SHUV strain 2504/3/14, neutralizing antibodies were only detectable in the serum of cattle C7, albeit at very low titres of 1/17 (14 dpi) and 1/24 (21 dpi), respectively (Table 2).

The results of the neutralization assay were confirmed by an indirect immunofluorescence assay. A fluorescence signal was visible for all cattle infected with SHUV strain 2162/16 from day 14 onwards, reaching the highest titres on day 21 (1/350). No fluorescence could be seen in samples of the cattle inoculated with SHUV strain 2504/3/14 or the control animals. The commercially available SBV antibody ELISA scored positive in three cattle inoculated with strain 2162/16 (C1, C3 and C6) at 14 and/or 21 dpi. No antibodies were detected in cattle inoculated with SHUV strain 2504/3/14 or the control animals (Table2).

3.4 | Histopathology and in situ hybridization

Histopathology revealed a mild (C2) to moderate (C1, C4, C6) non-suppurative meningoencephalitis in the animals, in which SHUV RNA was detected by real-time RT-PCR in samples of the central nervous system. The grey and white matter was equally affected by perivascular cuffing and glial nodule formation. The most consistent, moderate inflammation and glial reaction were recorded in

TABLE 2 Results of the serological tests

	0 dpi			7 dpi			14 dpi			21 dpi		
Animal ID	NT (ND_{50})	IIFT	ELISA	NT (ND_{50})	IIFT	ELISA	NT (ND_{50})	IIFT	ELISA	NT (ND_{50})	IIFT	ELISA
C1	<1/5	<1/50	87	**1/24**	<1/50	48	**1/57**	**1/100**	**36**	**1/57**	**1/200**	**40**
C2	<1/5	<1/50	104	**1/28**	<1/50	62	**1/191**	**1/100**	51	**1/270**	**1/200**	50
C3	<1/5	<1/50	92	<1/5	<1/50	66	**1/95**	**1/150**	**34**	**1/320**	**1/250**	42
C4	<1/5	<1/50	103	<1/5	<1/50	91	**1/57**	**1/50**	73	**1/80**	**1/150**	67
C5	<1/5	<1/50	100	**1/12**	<1/50	79	**1/160**	**1/100**	41	**1/135**	**1/300**	55
C6	<1/5	<1/50	103	**1/14**	<1/50	75	**1/328**	**1/300**	41	**1/226**	**1/350**	**40**
C7	<1/5	<1/50	96	<1/5	<1/50	86	**1/17**	<1/50	63	**1/24**	<1/50	67
C8	<1/5	<1/50	100	<1/5	<1/50	96	<1/5	<1/50	70	<1/5	<1/50	73
C9	<1/5	<1/50	95	<1/5	<1/50	89	<1/5	<1/50	90	<1/5	<1/50	91
C10	<1/5	<1/50	103	<1/5	<1/50	94	<1/5	<1/50	94	<1/5	<1/50	90
C11	<1/5	<1/50	99	<1/5	<1/50	93	<1/5	<1/50	92	<1/5	<1/50	99
C12	<1/5	<1/50	92	<1/5	<1/50	88	<1/5	<1/50	78	<1/5	<1/50	83
C13	<1/5	<1/50	99	<1/5	<1/50	83	<1/5	<1/50	80	<1/5	<1/50	85
C14	<1/5	<1/50	96	<1/5	<1/50	88	<1/5	<1/50	89	<1/5	<1/50	92

Note: Titres measured in a microneutralization test are indicated as ND_{50}. Results of the indirect immunofluorescence test are given as the highest dilution in which a fluorescent signal was visible. ELISA (ID Screen SBV competition multispecies, IDvet) results are indicated as the sample optical density (OD) relative to the negative control OD, values above 40% were considered negative. Positive results are shown in bold letters.

the periductal matter of the cerebral aqueduct (3 out of 4 animals). The spinal cord was mildly affected in all infected animals. The hippocampus and cerebellum showed mild to moderate lesions in 3 out of 4 animals. In individual cases, mild perivascular infiltrates or glial reaction was detected in the frontal or parietal lobe or in periventricular area of the lateral ventricle.

Consistently, perivascular infiltrates as well as glial nodules were composed of CD3-positive T-cells and Iba-1-labelled microglia/macrophages in comparable amounts. T-cells were also present in increased numbers, scattered within the grey and white matter. CD79a-positive B cells were only rarely detected. Representative lesions are shown in Figure 3. Apoptosis was not a significant feature with only scattered labelled cells (supplementary Figure S1). Further, astrogliosis was not identified; the number and distribution of GFAP-positive astrocytes did not differ between inoculated animals and the control (supplementary Figure S1). Neither haemorrhage, nor mineralization, nor demyelination, or loss of Nissl substance was found.

Shuni virus RNA was detected by in situ RNA hybridization, within the lesions in the periductal white matter of the cerebral aqueduct, phenotypically consistent with neuronal cell processes (Figure 4).

4 | DISCUSSION

The spread of SHUV from the African continent to Israel (Golender et al., 2015) or the unexpected emergence of SBV in Central Europe in 2011 (Hoffmann et al., 2012) proved the ability of Simbu serogroup viruses to cause large-scale epidemics after incursion into previously not affected areas (EFSA, 2012; Golender et al., 2018). When naïve, pregnant ruminants are infected, SHUV is known for its ability to cause severe congenital malformations, abortion, premature birth, mummification or stillbirth (Golender et al., 2015). However, during its spread through the Middle East, another clinical presentation became evident, when neurological signs and fatalities were described in young and adult cattle (Golender et al., 2019). In addition to ruminants, SHUV has been associated with neurological disease in other animals such as horses (van Eeden et al., 2012) and was detected in several other domestic and wildlife species (Steyn et al., 2020), demonstrating the broad host range of SHUV.

In our study, virus isolates obtained from representative cases of both clinical presentations from recent outbreaks in Israel, that is a malformed ovine foetus and a heifer showing neurological symptoms, were injected into cattle to compare the outcome under standardized experimental conditions. When comparing the two virus strains used in this study on a molecular level, few but crucial differences have been found. In the S segment, the sequences differ by only three nucleotides, which does not lead to changes of amino acids within the N protein (Golender et al., 2019). However, for the non-structural protein NSs, which is coded in an overlapping alternative reading frame (Walter & Barr, 2011), the varying nucleotide at position 50 in the NSs open reading frame ORF results in a stop codon in strain SHUV 2504/3/14 instead of a tryptophan in strain 2162/16 (Golender et al., 2016, 2019). In vitro, this mutation led to a loss of the protein function (Golender et al., 2016), that is to prevent the activation of the host's innate immune response of releasing interferons (Elliott & Blakqori, 2011). In this study, it was demonstrated by a lack of viremia in all inoculated animals that the NSs function of strain 2504/3/14 is also impaired in vivo. The inability of NSs deletion mutant viruses to induce viremia in interferon-competent mammalians was already demonstrated for

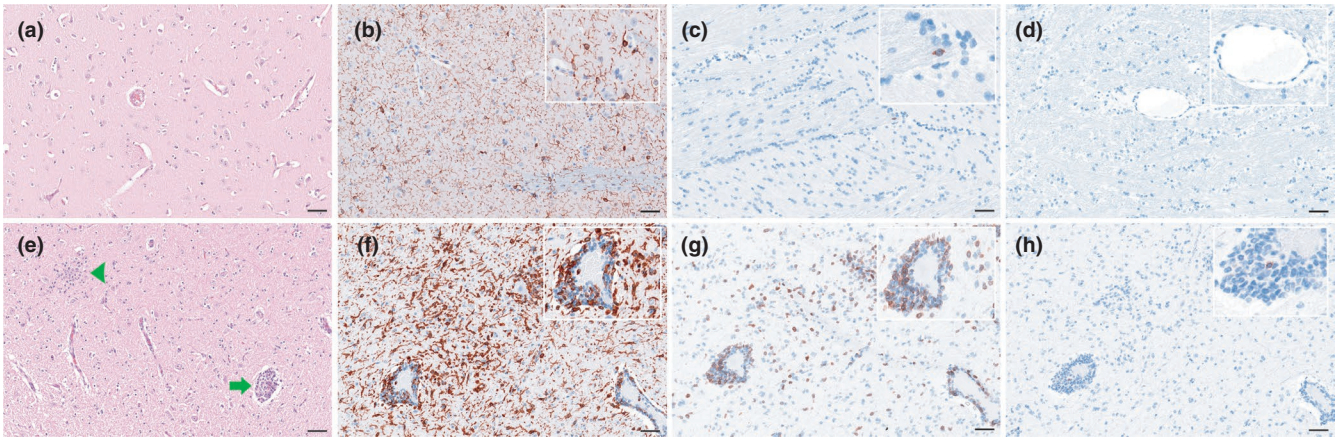

FIGURE 3 Histopathology and immunohistochemistry of brain sections of control (a-d) and Shuni virus-infected animals (e-h). Haematoxylin and eosin (a, e) or immunohistochemistry with AEC (red-brown) chromogen and Mayer's haematoxylin counterstain (b-d, f-h). All scale bars 50 μm, inlays showing details. (a) Unaffected brain, control animal. (b) Iba-1 labelled microglia/macrophages, note the equal distribution of slender cells, control animal. (c) CD3-positive, single cell, control animal. (d) Absence of CD79a-labelled B cells, control animal. (e) Non-suppurative, moderate encephalitis with mononuclear, perivascular cuffing (arrow, 4 layers) and focal glial nodule formation (arrow head), infected animal C6, (f) Iba-1-positive microglial cells/macrophages, note the increased number (hyperplasia) and size (hypertrophy) of labelled cells, infected animal C4. (g) CD3-positive cells in high number, perivascularly and scattered within the neuropil, infected animal C4. (h) CD79a labelled, single B-cell, infected animal C4 [Colour figure can be viewed at wileyonlinelibrary.com]

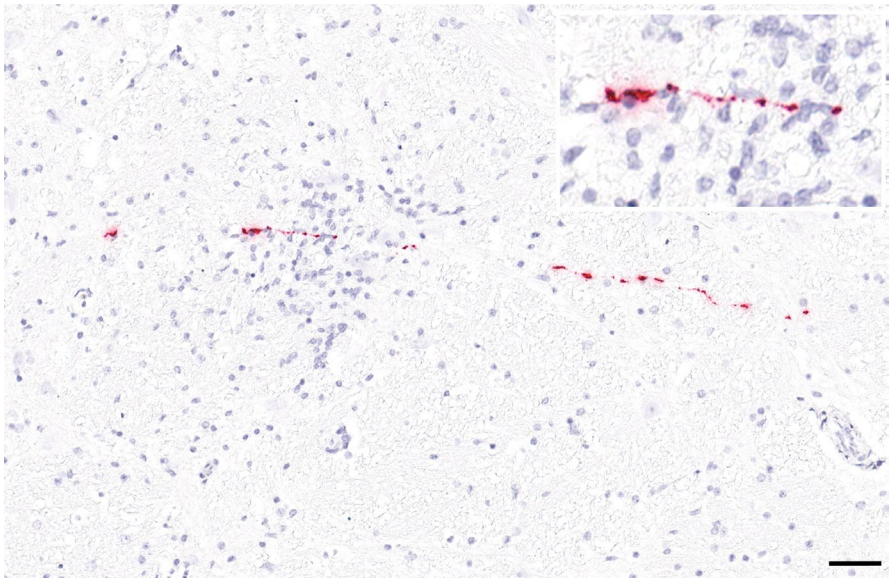

FIGURE 4 RNA in situ hybridization of Shuni virus (SHUV)-infected animal C4. Chromogenic labelling (fast red) with probes to SHUV N-coding region are visible intralesional, in neuronal cell body processes (arrow and inlay), within a focal inflammatory reaction, Mayer's haematoxylin counterstain. Scale bar = 50 μm [Colour figure can be viewed at wileyonlinelibrary.com]

other simbuviruses, such as SBV (Kraatz et al., 2015). However, for SBV, the NSs deletion mutant was generated by reverse genetics (Kraatz et al., 2015), while the SHUV mutant used in this study evolved naturally. This mutant virus occurred in a malformed foetus and not in an acutely infected adult animal, further supporting the theory that genetically highly variable Simbu serogroup viruses evolving in foetuses represent dead-end artefacts that are not fit for the usual transmission cycle. Nevertheless, the inoculation of strain 2504/4/14 led to the development of neutralizing antibodies in one of six animals, albeit at low level, which has been likewise described for an NSs-deleted SBV mutant (Kraatz et al., 2015). In the case of SBV, this was used for the generation of live attenuated candidate vaccines, since immunization with the NSs deletion mutant conferred protection from virulent virus challenge. Whether this holds also true for the naturally evolved SHUV strain needs to be further evaluated in future vaccination-challenge experiments.

In contrast to the NSs-deficient virus, SHUV strain 2162/16, which was isolated from an acutely infected animal, successfully infected calves leading to a short-lived viremia and seroconversion in all six inoculated animals. This, for vector-transmitted agents surprisingly short viremia, was also demonstrated for other simbuviruses such as SBV (Hoffmann et al., 2012) and AKAV (Lee et al., 2016) and seems to be long enough for the arthropod vector to acquire the virus and for the establishment of a successful transmission cycle between the vector and the mammalian hosts.

Even though experimentally infected animals did not show clinical signs characteristic for a neurological disease, viral genome was detected in the central nervous system of four out of six animals by real-time RT-PCR. Furthermore, the histopathological investigation revealed a non-suppurative meningoencephalitis in all of these animals. Perivascular cuffs and glial nodules as common characteristic features of viral encephalitis were observed in both, naturally infected (Golender et al., 2019) and in experimentally inoculated cattle. In addition, SHUV RNA was visualized in this study within the lesions by in situ hybridization. Hence, SHUV could be determined as the causative agent of the encephalitis.

In general, the clinical picture observed in SHUV infected cattle mirrors that of the related AKAV, where some strains may induce encephalitis in postnatally infected cattle, while others are associated with abnormal deliveries (Yanase et al., 2018). However, AKAV strains found in association with encephalitis were also isolated from asymptomatic cattle (Yanase et al., 2018), and SHUV isolates likewise did not reveal any specific genomic changes that could be associated with neuropathogenicity (Golender et al., 2019).

As acute SHUV infections often seem to be asymptomatic or associated with only mild, unspecific clinical signs, the spatial distribution of the virus might be underestimated. As demonstrated in this study, even major histological findings like encephalitis might not result in symptoms. To identify the actual distribution of SHUV, serological screenings might be considered, especially since the detection of the virus itself is time restricted by the short viremia of only a few days. Both assays presented in this study, that is the neutralization test and the indirect immunofluorescence test, proved suitable for the detection of SHUV antibodies. Alternatively, biting midges (genus *Culicoides*) could be monitored for the presence of viral genome as has been demonstrated for various Simbu serogroup viruses (Behar et al., 2020; De Regge et al., 2012; Stram et al., 2004).

In summary, it was demonstrated that cattle, one of the major target species of SHUV, represent a suitable animal model to study the pathogenesis of the virus. Moreover, the neuropathogenicity of SHUV could be demonstrated under experimental conditions. Thus, SHUV should be included in the list of differential diagnosis of encephalitis in ruminants and an outbreak of SHUV in Europe would most likely result in more infected species and a broader spectrum of clinical signs, including neuropathology.

ACKNOWLEDGEMENTS

We thank Bianka Hillmann and Silvia Schuparis for their excellent technical assistance and the animal caretakers for their dedicated

work. This study was funded by the German Federal Ministry of Food and Agriculture (BMEL) through the Federal Office for Agriculture and Food (BLE), grant number 281B101816, and by the Marie Skłodowska-Curie Actions (MSCA) Innovative Training Networks (ITN) H2020-MSCA-ITN-2016, grant agreement number 721367. Open access funding enabled and organized by Projekt DEAL.

CONFLICT OF INTEREST

The authors declare no conflict of interest.

ETHICAL APPROVAL

The experimental protocol was evaluated by a state ethics commission and approved by the competent authority (permission number LALLF M-VTSD/7221.3–2-010/18).

DATA AVAILABILITY STATEMENT

The data that support the findings of this study are available from the corresponding author upon reasonable request.

ORCID

Martin Beer https://orcid.org/0000-0002-0598-5254
Kerstin Wernike https://orcid.org/0000-0001-8071-0827

REFERENCES

Beer, M., & Wernike, K. (2019). Akabane virus and Schmallenberg virus. *Reference Module in Life Sciences*, https://doi.org/10.1016/b978-0-12-809633-8.20939-4

Behar, A., Rot, A., Lavon, Y., Izhaki, O., Gur, N., & Brenner, J. (2020). Seasonal and spatial variation in Culicoides community structure and their potential role in transmitting Simbu serogroup viruses in Israel. *Transboundary and Emerging Diseases*, *67*(3), 1222–1230. https://doi.org/10.1111/tbed.13457

Behrens, B., & Kärber, G. (1934). Wie sind Reihenversuche für biologische Auswertungen am zweckmäßigsten anzuordnen? *Naunyn-Schmiedebergs Archiv Für Experimentelle Pathologie Und Pharmakologie*, *177*(2), 379–388. https://doi.org/10.1007/BF02023142

Causey, O. R., Kemp, G. E., Causey, C. E., & Lee, V. H. (1972). Isolations of Simbu-group viruses in Ibadan, Nigeria 1964–69, including the new types Sango, Shamonda, Sabo and Shuni. *Annals of Tropical Medicine and Parasitology*, *66*(3), 357–362. https://doi.org/10.1080/00034983.1972.11686835

De Regge, N., Deblauwe, I., De Deken, R., Vantieghem, P., Madder, M., Geysen, D., & Cay, A. B. (2012). Detection of Schmallenberg virus in different Culicoides spp. by real-time RT-PCR. *Transboundary and Emerging Diseases*, *59*(6), 471–475. https://doi.org/10.1111/tbed.12000

EFSA (2012). *"Schmallenberg" virus: analysis of the epidemiological data* (November 2012). EFSA Supporting Publications 2012. EN-360. http://www.efsa.europa.eu/en/supporting/doc/360e.pdf; accessed 15/07/2013.

Elliott, R. M., & Blakqori, G. (2011). Molecular biology of orthobunyaviruses. In A. Plyusnin, & R. M. Elliott (Eds.), *Bunyaviridae: Molecular and Cellular Biology*. Caister Academic Press.

Golender, N., Brenner, J., Valdman, M., Khinich, Y., Bumbarov, V., Panshin, A., Edery, N., Pismanik, S., & Behar, A. (2015). Malformations Caused by Shuni Virus in Ruminants, Israel, 2014–2015. *Emerging Infectious Diseases*, *21*(12), 2267–2268. https://doi.org/10.3201/eid2112.150804

Golender, N., Bumbarov, V., Assis, I., Beer, M., Khinich, Y., Koren, O., Edery, N., Eldar, A., & Wernike, K. (2019). Shuni virus in Israel: Neurological disease and fatalities in cattle. *Transboundary and Emerging Diseases*, *66*(3), 1126–1131. https://doi.org/10.1111/tbed.13167

Golender, N., Bumbarov, V. Y., Erster, O., Beer, M., Khinich, Y., & Wernike, K. (2018). Development and validation of a universal S-segment-based real-time RT-PCR assay for the detection of Simbu serogroup viruses. *Journal of Virological Methods*, *261*, 80–85. https://doi.org/10.1016/j.jviromet.2018.08.008

Golender, N., Wernike, K., Bumbarov, V., Aebischer, A., Panshin, A., Jenckel, M., Khinich, Y., & Beer, M. (2016). Characterization of Shuni viruses detected in Israel. *Virus Genes*, *52*(6), 806–813. https://doi.org/10.1007/s11262-016-1381-3

Hoffmann, B., Scheuch, M., Höper, D., Jungblut, R., Holsteg, M., Schirrmeier, H., Eschbaumer, M., Goller, K. V., Wernike, K., Fischer, M., Breithaupt, A., Mettenleiter, T. C., & Beer, M. (2012). Novel orthobunyavirus in Cattle, Europe, 2011. *Emerging Infectious Diseases*, *18*(3), 469–472. https://doi.org/10.3201/eid1803.111905

Kirkland, P. D. (2015). Akabane virus infection. *Revue Scientifique Et Technique*, *34*(2), 403–410. https://doi.org/10.20506/rst.34.2.2366

Kraatz, F., Wernike, K., Hechinger, S., König, P., Granzow, H., Reimann, I., & Beer, M. (2015). Deletion mutants of Schmallenberg virus are avirulent and protect from virus challenge. *Journal of Virology*, *89*(3), 1825–1837. https://doi.org/10.1128/JVI.02729-14

Lee, H., Jeong, H., Park, S., Yang, M.-S., Kim, J., Bae, J., Kwon, Y., Kim, M.-S., Oem, J.-K., Lee, M.-H., Lim, C.-W., & Kim, B. (2016). Experimental infection of cows with newly isolated Akabane virus strain (AKAV-7) causing encephalomyelitis. *Veterinary Research*, *47*(1), 62. https://doi.org/10.1186/s13567-016-0349-6

Miyazato, S., Miura, Y., Hase, M., Kubo, M., Goto, Y., & Kono, Y. (1989). Encephalitis of cattle caused by Iriki isolate, a new strain belonging to Akabane virus. *Nihon Juigaku Zasshi*, *51*(1), 128–136. https://doi.org/10.1292/jvms1939.51.128

Möhlmann, T. W. R., Oymans, J., Wichgers Schreur, P. J., Koenraadt, C. J. M., Kortekaas, J., & Vogels, C. B. F. (2018). Vector competence of biting midges and mosquitoes for Shuni virus. *PLoS Neglected Tropical Diseases*, *12*(12), e0006993. https://doi.org/10.1371/journal.pntd.0006993

Moore, D. L., Causey, O. R., Carey, D. E., Reddy, S., Cooke, A. R., Akinkugbe, F. M., David-West, T. S., & Kemp, G. E. (1975). Arthropod-borne viral infections of man in Nigeria, 1964–1970. *Annals of Tropical Medicine and Parasitology*, *69*(1), 49–64. https://doi.org/10.1080/00034983.1975.11686983

Oluwayelu, D., Wernike, K., Adebiyi, A., Cadmus, S., & Beer, M. (2018). Neutralizing antibodies against Simbu serogroup viruses in cattle and sheep, Nigeria, 2012–2014. *BMC Veterinary Research*, *14*(1), 277. https://doi.org/10.1186/s12917-018-1605-y

Plyusnin, A., & Elliott, R. M. (2011). *Bunyaviridae : Molecular and cellular biology*. Caister Academic Press.

Steyn, J., Motlou, P., van Eeden, C., Pretorius, M., Stivaktas, V. I., Williams, J., Snyman, L. P., Buss, P. E., Beechler, B., Jolles, A., Perez-Martin, E., Myburgh, J. G., Steyl, J., & Venter, M. (2020). Shuni Virus in Wildlife and Nonequine Domestic Animals, South Africa. *Emerging Infectious Diseases*, *26*(7), 1521–1525. https://doi.org/10.3201/eid2607.190770

Stram, Y., Brenner, J., Braverman, Y., Banet-Noach, C., Kuznetzova, L., & Ginni, M. (2004). Akabane virus in Israel: A new virus lineage. *Virus Research*, *104*(1), 93–97. https://doi.org/10.1016/j.virusres.2004.03.004

Toussaint, J. F., Sailleau, C., Breard, E., Zientara, S., & De Clercq, K. (2007). Bluetongue virus detection by two real-time RT-qPCRs targeting two different genomic segments. *Journal of Virological Methods*, *140*(1–2), 115–123. https://doi.org/10.1016/j.jviromet.2006.11.007

van Eeden, C., Swanepoel, R., & Venter, M. (2014). Antibodies against West Nile and Shuni Viruses in Veterinarians, South Africa. *Emerging Infectious Diseases*, *20*(8), 1409–1411. https://doi.org/10.3201/eid2008.131724

van Eeden, C., Williams, J. H., Gerdes, T. G., van Wilpe, E., Viljoen, A., Swanepoel, R., & Venter, M. (2012). Shuni virus as cause of neurologic disease in horses. *Emerging Infectious Diseases*, *18*(2), 318–321. https://doi.org/10.3201/eid1802.111403

Walter, C. T., & Barr, J. N. (2011). Recent advances in the molecular and cellular biology of bunyaviruses. *Journal of General Virology*, *92*, 2467–2484. https://doi.org/10.1099/vir.0.035105-0

Wernike, K., Beer, M., & Hoffmann, B. (2017). Schmallenberg Virus Infection Diagnosis: Results of a German Proficiency Trial. *Transboundary and Emerging Diseases*, *64*(5), 1405–1410. https://doi.org/10.1111/tbed.12517

Wernike, K., Elbers, A., & Beer, M. (2015). Schmallenberg virus infection. *Revue Scientifique Et Technique*, *34*(2), 363–373. https://doi.org/10.20506/rst.34.2.2363

Yanase, T., Kato, T., Hayama, Y., Akiyama, M., Itoh, N., Horiuchi, S., Hirashima, Y., Shirafuji, H., Yamakawa, M., Tanaka, S., & Tsutsui, T. (2018). Transition of Akabane virus genogroups and its association with changes in the nature of disease in Japan. *Transboundary and Emerging Diseases*, *65*(2), e434–e443. https://doi.org/10.1111/tbed.12778

SUPPORTING INFORMATION

Additional supporting information may be found online in the Supporting Information section.

How to cite this article: Sick F, Breithaupt A, Golender N, Bumbarov V, Beer M, Wernike K. Shuni virus-induced meningoencephalitis after experimental infection of cattle. *Transbound. Emerg. Dis.*2021;68:1531–1540. https://doi.org/10.1111/tbed.13823